Advances in Engineering Software 149 (2020) 102864

Contents lists available at ScienceDirect

Advances in Engineering Software

journal homepage: www.elsevier.com/locate/advengsoft

Research on parameterization and optimization procedure of low-Reynolds-number airfoils based on genetic algorithm and Bezier curve

Xuesong Wei[a], Xiaoyang Wang[a], Songying Chen[a,*]

[a] Key Laboratory of High Efficiency and Clean Mechanical Manufacture of Ministry of Education, National Demonstration Center for Experimental Mechanical Engineering Education, School of Mechanical Engineering, Shandong University, Jinan, Shandong, 250061, China

ARTICLE INFO

Keywords:
Parameterization
Multi-objective optimization
Airfoil
NSGA II
Bezier curve

ABSTRACT

A systematic procedure of high-precision parameterization and multi-objective optimization for airfoils was proposed in this paper in order to improve the aerodynamic performance under full working conditions. The Bezier curve was applied in the airfoil parameterization with the coordinates of the 8 Bezier control points chosen to be the design variables. The control points were initialized by self-programming software and then optimized by direct search method to guarantee the fitting precision. The multi-objective optimization of low-Reynolds-number airfoil E387 was executed through NSGA II based on the result from XFOIL calculation, with the increment and variance of lift-drag ratio chosen to be the objective functions. Two representative solutions were selected from the Pareto front, and the performances of the new airfoils were promoted in different ways. The lift-drag ratio of the optimized airfoil with smaller variance is increased uniformly under different attack angles and maintains the similar characteristics with the original one. For the optimized airfoil with larger variance, the distribution of lift-drag ratio relative to the attack angle is altered obviously, and the performance under small attack angles and stall conditions are significantly ameliorated. The introduction of variance control in the objective function enables the differentiation of the optimized solutions for different requirement in engineering application.

1. Introduction

Airfoils are the key components in turbines and aircrafts in order to generate lift forces and extract energy, and the performance of the airfoil is significantly effective to the performance of the whole unit. Consequently, the first step of the entire design is always the optimization of the airfoil, which belongs to the multi-objective problem where various conditions have to be considered. The Genetic Algorithm has been widely applied in recent research of multi-objective optimization of airfoils.

In the research of airfoils for turbines, Bedon [1] and Daróczy L [2] adopted genetic algorithm in the optimization of Darrieus wind turbines, and successfully obtained an airfoil shape which outperforms the original airfoils. Luo [3] conducted an optimization of hydrofoils for marine current turbine by genetic algorithm NSGA-II (Non-Dominated Sorting Genetic Algorithm II) to enhance lift-drag ratio and cavitation performance. The distance metric in the metric space was introduced to reduce the number of objective functions and three optimized hydrofoils with different performance characteristics were obtained for different specific requirements. Jeong J H [4] conducted the optimization of the thick airfoils for wind turbines using genetic algorithm, and improved the lift-to-drag ratio by 30%~40% compared with the original ones. Huang [5] developed a series of fully symmetrical hydrofoils with various relative thickness using genetic algorithm NSGA-II to comprise optimized blade profiles for bi-directional counter-rotating tidal turbine. The hydrodynamic performance was improved significantly for both hydrofoils and tidal turbines. Ram K R [6] generated airfoil sections for a 20 kW wind turbine with high resistance to soiling effects using Genetic Algorithm, a net improvement of 2.3% is achieved in the turbine's annual energy production and the power output can still remain stable even in soiled or dirty conditions.

In the research of airfoils for aircrafts, Zhang [7] developed an optimized airfoil based on NACA 0012 by coupling multi-island genetic algorithm (MIGA) with nonlinear programming by quadratic Lagrangian (NLPQL), and the combination of the two optimization methods achieved better results than the methods used separately. Jones [8] applied genetic algorithm in the optimization of an helicopter rotor airfoil to minimize the drag and overall noise, and the new airfoil shapes provided starting points for further application. Obayashi [9] designed an inverse optimization method coupled with MIGA to

* Corresponding author.
E-mail address: chensy66@sdu.edu.cn (S. Chen).

https://doi.org/10.1016/j.advengsoft.2020.102864
Received 17 March 2020; Received in revised form 25 May 2020; Accepted 12 June 2020

Nomenclature

c	chord length
C_l	lift coefficient
C_d	drag coefficient
C_l/C_d	lift-drag ratio
α	attack angle
C_p	pressure coefficient
Ma	Mach number
Re	Reynolds number

generate a transonic wing for mid-size regional aircraft with improved pressure distributions and enforced straight isobar pattern on the upper surface of the wing. Liu [10] utilized Controlled Elitist NSGA-II to design an optimized airfoil for nano rotor blade with excellent aerodynamic performance at ultra-low Reynolds number.

The research mentioned above covered various research areas from turbines to aircrafts, and enriched the application of genetic algorithm in the multi-objective optimization of airfoils, which is of great significance to engineering application. The optimization method introduced in this research, however, is different from the previous investigations. The present research is focused on the aerodynamic performance under full conditions (with large range of attack angles) of low-Reynolds-number high-lift airfoils. The concept of variance was introduced to control the distribution of lift-drag ratio relative to the attack angle in order to improve the aerodynamic characteristics under different conditions. The rapid optimization procedure was constructed according to these intentions and can be coupled with other design and optimization procedures.

The mostly adopted method of performance calculation in optimization researches is CFD (Computational Fluid Dynamics). In order to calculate the fitness of the objective function for each individual in the evolving group, the genetic algorithm requires frequent calls for computing resources, and the numerical solution of the Navier-Stokes equations will make the calculation complexity increase exponentially, which is disadvantageous to engineering application. In this case, the reduction of the amount of calculation and improvement of efficiency are of vital importance to the optimization of airfoils. The strategy generally adopted is the application of approximate model such as neural network or response surface function. This type of model is able to avoid the occupation of large amount of computational resources for flow field calculation, but the calculation error will be inevitably non-ignorable with the increasing of parameter variables and the accuracy of final result might be affected.

In addition to CFD calculations, the XFOIL program [11,12] provides an alternative method of obtaining airfoil aerodynamic data. The XFOIL program combines the vortex panel method with the boundary layer theory to enhance calculating speed with acceptable precision. Molland [13] calculated the lift drag ratio and cavitation performance of 4 kinds of NACA airfoils using XFOIL code, and the calculated result was in good agreement with the experimental data. Morgado [14] compared the results of XFOIL program with CFD. The results showed that the XFOIL program possesses good accuracy in the calculation of low-Reynolds-number airfoils, and can be adopted in the rapid design. The application of XFOIL code in other researches has also obtained desirable results [15–17].

Based on these considerations, XFOIL program is introduced to couple with genetic algorithm instead of CFD method in the present research. The multi-objective optimization is conducted using ISIGHT [18] , which is a generic software framework for integration, automation, and optimization of design processes, widely applied in aviation, power, electronics and other industries. In this paper, the ISIGHT platform is coupled with the XFOIL program and genetic algorithm NSGA-II to finish the multi-objective optimization of airfoil E387, which is a typical representative of low-Reynolds-number airfoil. As the pre-processing module of the optimization, a rapid high-precision parameterization procedure coupled with direct search method is also introduced, so the closed-loop solution for airfoil design and optimization is provided.

2. Airfoil parameterization

2.1. Bezier curve

The parameterization method of airfoils has significant effect on performance calculation. The Bezier curve has excellent geometric characteristics, which is very suitable for the geometric description of airfoils [19], and hence is applied in the present research. The expression of Bezier curve of nth order is as follows:

$$P(t) = \sum_{i=0}^{n} B_{i,n} Q_i = \sum_{i=0}^{n} C_n^i (1-t)^{n-i} t^i Q_i \tag{1}$$

Where $P(t)$ is an arbitrary point on the curve to be described, and t is parametric variable ($t \in (0, 1)$). $B_{i,\ n}$ is the Bernstein basis function, $C_n^i$is the combination number, Q_i is the control point of Bezier curve. In this paper, Bezier curves of 5th order were adopted to fit the upper and lower surfaces of the airfoil E387. The procedure is composed of two sections: fitting initialization and fitting optimization. The first section produces the preliminary control point coordinates, and the second section obtains the final coordinates with high fitting precisions. The detailed description is as follows.

2.2. Fitting initialization

In this section, the preliminary control point coordinates are generated to provide database for the second section, and there are no strict requirements for precision. In the present research, a self-developed software ‘Bezier Curve Fitting.exe’ is applied to this task, and the software interface and function is shown in Fig. 1.

This software is developed based on Basic language, and is able to provide convenient operation interface of airfoil fitting. Those square sliders shown in Fig. 1(a) represent Bezier control points which can be easily moved according to the profile of the curve to be fitted (the red curve in Fig. 1(a)). The fitting result (the blue curve in Fig. 1(a)) will be calculated by Bezier function and displayed simultaneously. After the rapid adjustment of control point position, the fitting result can be generated.

The upper and lower curves of airfoil E387 are fitted separately by 5th order Bezier curves, and the result is shown in Fig. 2. The coordinates have been normalized in terms of chord length c, and P0-P9 are the control points. It can be seen that the profile has already been fitted properly from the visual perspective. The curve deviation analysis function of the UG is adopted to calculate the deviations of the fitted curves, which are displayed in Fig. 3. Because the airfoil profile data has been normalized, the deviations are also normalized values. In Fig. 3, the coordinate of 0 in x-axis represents the leading edge while the coordinate of 1 in x-axis represents the trailing edge. The average and maximum deviation for the upper curve is 0.000265 and 0.000638 respectively, and the average and maximum deviation for the lower curve is 0.000049 and 0.000113 respectively. In order to further reduce fitting deviation and improve accuracy, the fitting optimization is carried out in the next section.

2.3. Fitting optimization

Based on the initial control points generated in the previous section, the single-objective optimization procedure for lower deviations is

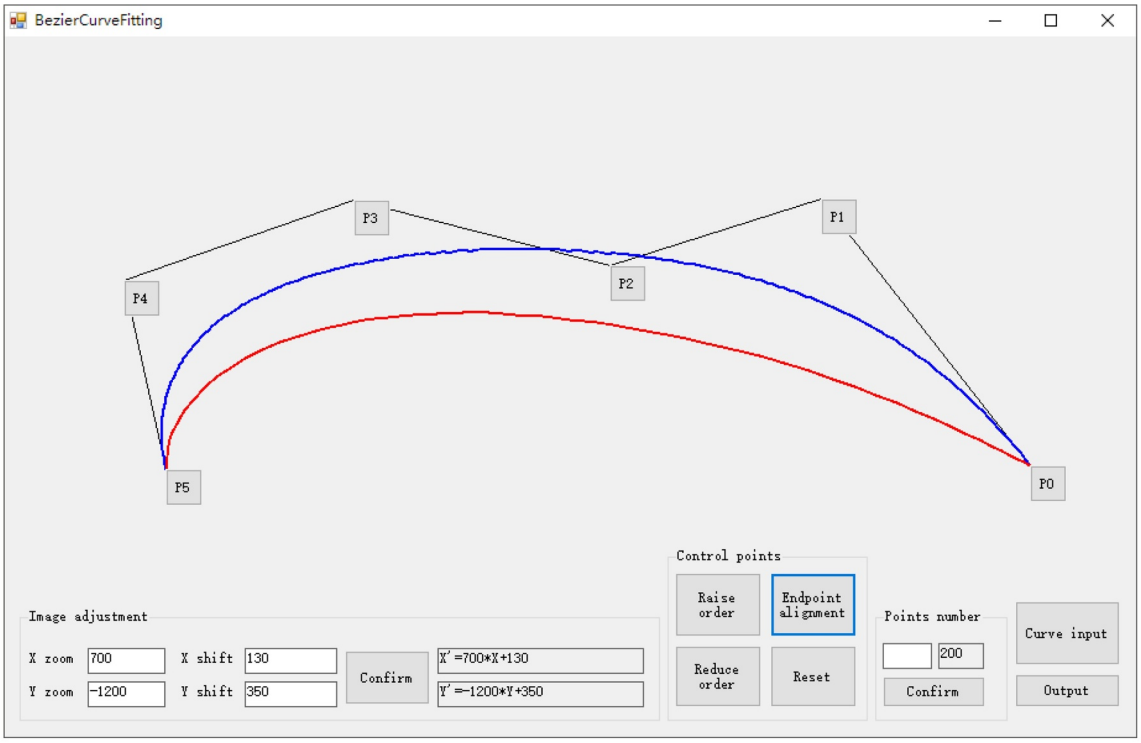

(a) Interface illustration

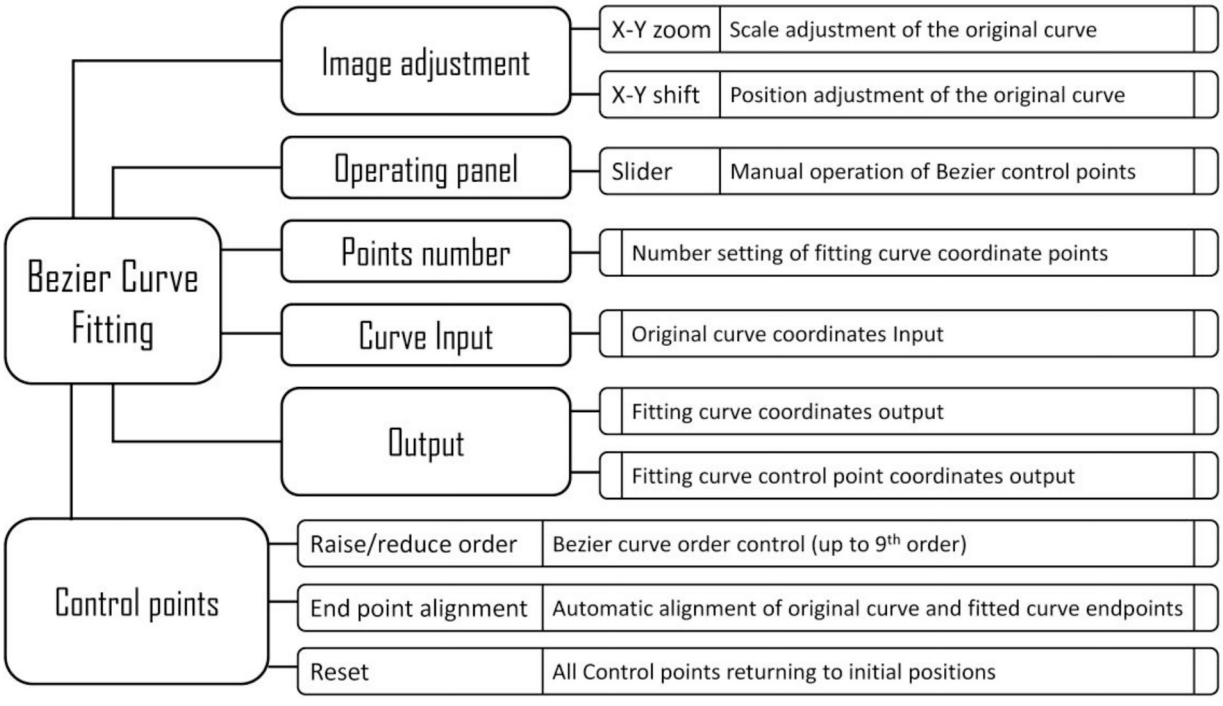

(b) Function illustration

Fig. 1. Interface and function illustration of self-programming software 'Bezier Curve Fitting'. (a) Interface illustration, (b) Function illustration.

constructed in this section. The objective function is the sum of squares of deviations which is calculated by another self-developed program 'BezierDeviation.exe'. The calculating procedure is illustrated in Fig. 4.

In Fig. 4, k represents the total number of points to be examined on the original upper curve ($k = 30$) and lower curve ($k = 27$) of airfoil E387. The X equation and Y equation are derived from Eq. (1).

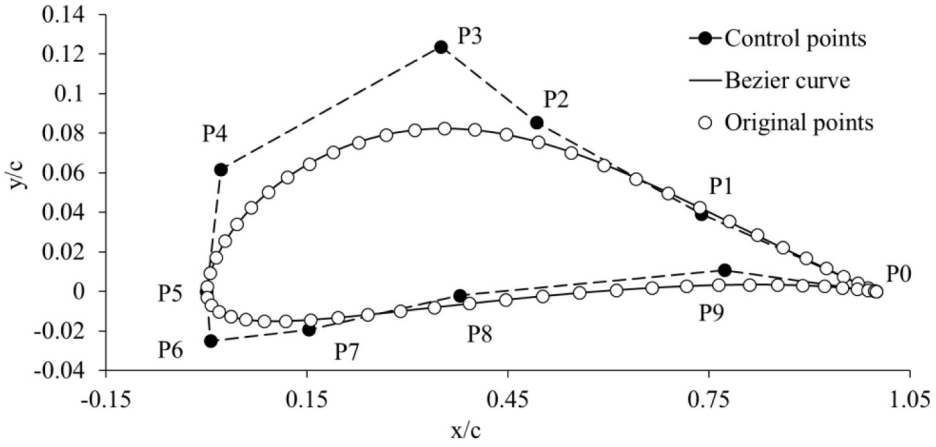

Fig. 2. Initial Fitted curves of airfoil E387.

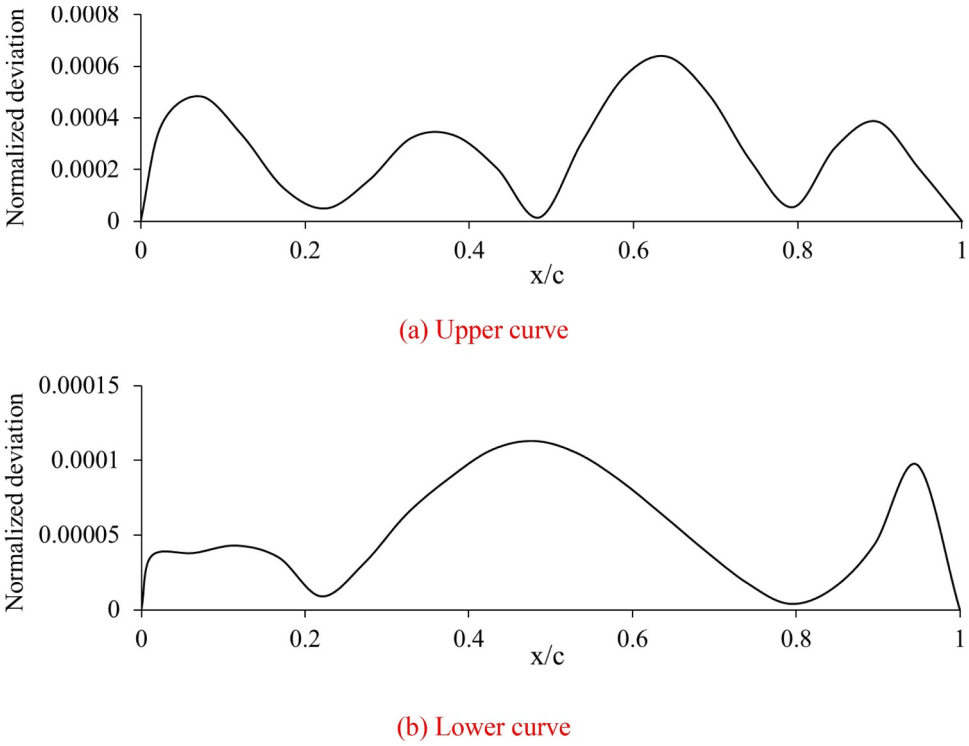

Fig. 3. Normalized deviation check of the initial fitted curves of airfoil E387. (a) Upper curve, (b) Lower curve.

$$X(t) = \sum_{i=0}^{n} B_{i,n} X_i^c = \sum_{i=0}^{n} C_n^i (1-t)^{n-i} t^i X_i^c \tag{2}$$

$$Y(t) = \sum_{i=0}^{n} B_{i,n} Y_i^c = \sum_{i=0}^{n} C_n^i (1-t)^{n-i} t^i Y_i^c \tag{3}$$

Where X^c and Y^c represent the x and y coordinate of control point. The other parameters are the same with Eq. (1).

The variables are the coordinates of control points, with the range shown in Table 1 (P0 and P5 are kept unchanged). Two direct search algorithms (Hooke-Jeeves method [20] and Downhill Simplex method [21]) are separately investigated. Direct search algorithms can effectively explore the local area around the initial design point, but the optimization result is affected by the initial data, which is the reason for the existence of the initial fitting. The maximum iterations for Downhill Simplex method are set as 1000, and the maximum evaluations for Hooke-Jeeves method are set as 1000. The other parameters are set as default values.

The Downhill Simplex method got the optimal solution for upper and lower curve at the 607th and the 799th run respectively, while Hooke-Jeeves method got the optimal solution for upper and lower curve at the 868th and the 861th run respectively. The optimization

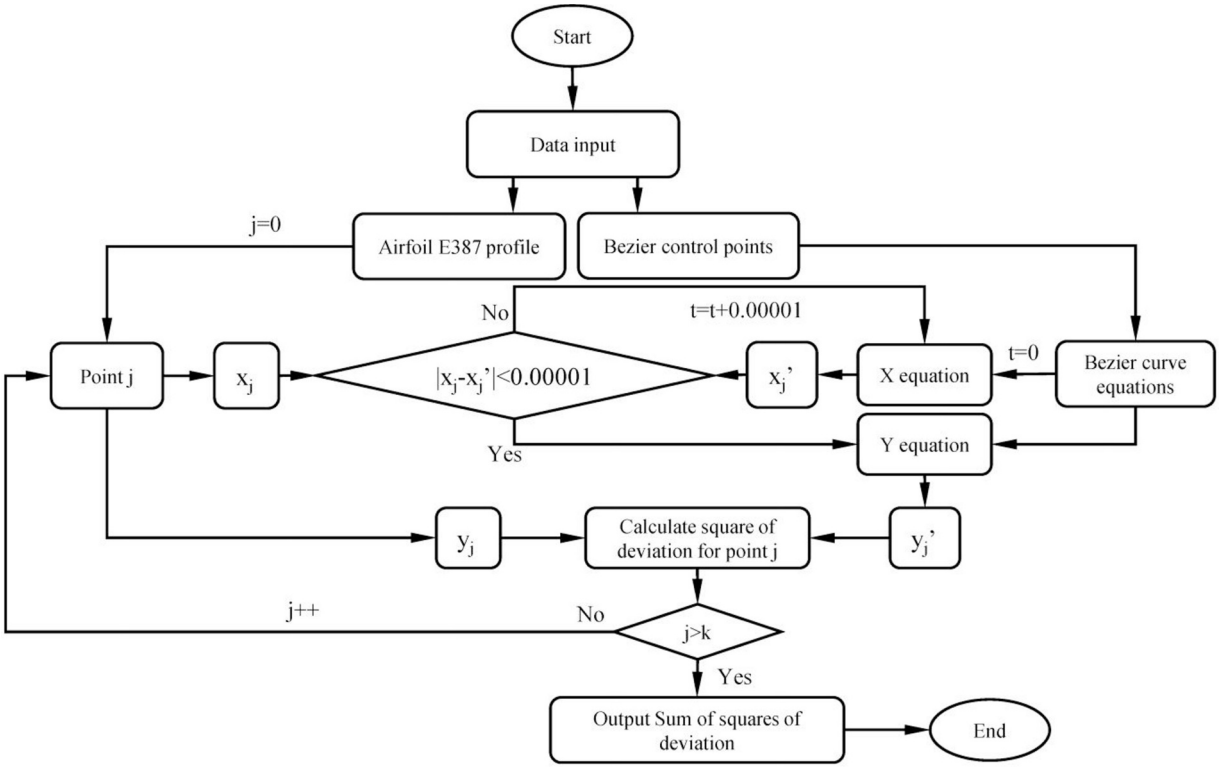

Fig. 4. The flow chart of deviation calculation.

Table 1
Variation rang of control points coordinates.

Control points for upper curve	Lower limit	Initial value	Upper limit	control points for lower curve	Lower limit	Initial value	Upper limit
P1*x*	0.639	0.738571429	0.839	P6*x*	−0.094	0.005714286	0.106
P1*y*	0.019	0.039142857	0.059	P6*y*	−0.045	−0.025000000	−0.005
P2*x*	0.393	0.492857143	0.593	P7*x*	0.053	0.152857143	0.253
P2*y*	0.065	0.085428571	0.105	P7*y*	−0.039	−0.019250000	0.001
P3*x*	0.250	0.350000000	0.450	P8x	0.279	0.378571429	0.479
P3*y*	0.104	0.123714286	0.144	P8*y*	−0.022	−0.002083333	0.018
P4*x*	−0.079	0.021428571	0.121	P9*x*	0.673	0.772857143	0.873
P4*y*	0.042	0.061714286	0.082	P9*y*	−0.009	0.010750000	0.031

process is shown in Fig. 5. The deviations of the two algorithms are shown in Fig. 6 with detailed quantitative comparison shown in Table 2. The two methods have both obtained much better results than initial fitting, the maximum deviations for the upper curve are below 0.00024, and the maximum deviations for the lower curve are below 0.00007, which is accurate enough for engineering research. The fitting effect of Downhill Simplex method is slightly better than that of Hooke-Jeeves method. As a result, the control points from downhill simplex method (displayed in Fig. 7 and Table 3) are chosen to be the starting points for the next investigation.

3. Multi-objective optimization of aerodynamic performance

3.1. Genetic algorithm

The genetic algorithm is a global optimization method proposed by Professor Holland [22] of Stanford University in the 1970s based on Darwin's theory of evolution and Mendel's theory of gene to simulate the principle of survival of the fittest. The genetic algorithm starts with a population consisting of a number of individuals encoded by genes to represent a set of possible solutions. In each generation, the individuals are selected according to the fitness in the problem domain with the crossover and mutation of the genes to produce the new generation. After many generations of evolution, the adaptability of the population will gradually increase. In this paper, the optimization process was conducted by Non-Dominated Sorting Genetic Algorithm II (NSGA II) [23] which introduces fast non-dominated sorting and congestion mechanism to drive the evolutionary process to converge to the frontiers and protect the diversity of the Pareto optimal solutions at the same time. The excellent individuals of the parent generation are preserved by elitist strategy in order to prevent the loss of Pareto optimal solutions.

3.2. Optimization procedure

The optimization target is airfoil E387, and the coordinates of 8 control points (P1-P4 for the upper curve and P6-P9 for the lower curve) are chosen to be the design variables with their variation ranges

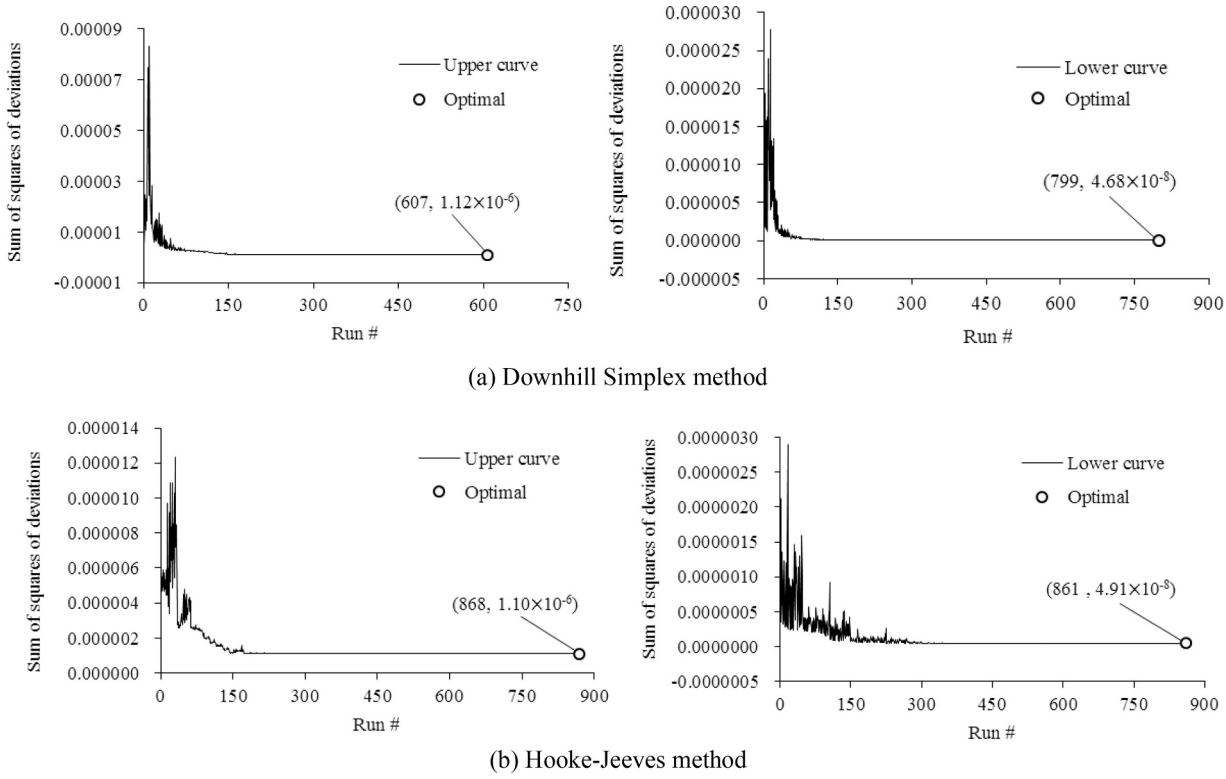

Fig. 5. The optimization process of two methods. (a) Downhill Simplex method, (b) Hooke-Jeeves method.

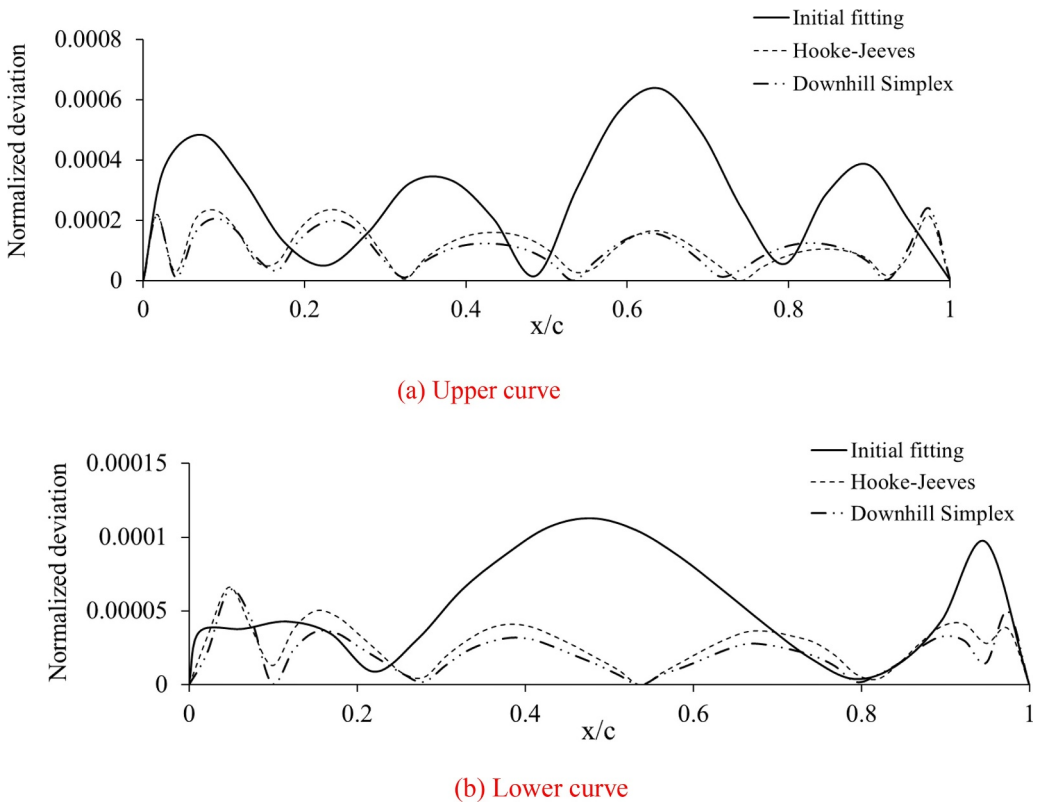

Fig. 6. Normalized deviations comparison between the initial and optimized fitted curves of airfoil E387. (a) Upper curve, (b) Lower curve.

Table 2
Deviation comparison between different algorithms.

	Method	Maximum deviation		Average deviation	
Upper curve	Initial fitting	0.000638		0.000265	
	Hooke-Jeeves	0.000234	↓63.3%	0.000110	↓58.6%
	Downhill Simplex	0.000239	↓62.5%	0.000100	↓62.3%
Lower curve	Initial fitting	0.000113		0.000049	
	Hooke-Jeeves	0.000067	↓41.0%	0.000027	↓46.3%
	Downhill Simplex	0.000064	↓43.4%	0.000021	↓57.5%

Table 3
Control points coordinates of airfoil E387 by Downhill Simplex method.

control points for upper curve	Optimized value	control points for lower curve	Optimized value
P1x	0.773969293	P6x	−0.001073036
P1y	0.036122616	P6y	−0.025062025
P2x	0.463096708	P7x	0.186959028
P2y	0.082727179	P7y	−0.019384850
P3x	0.393964529	P8x	0.327455044
P3y	0.125631601	P8y	−0.001939915
P4x	0.014162857	P9x	0.799243450
P4y	0.063724995	P9y	0.010752819

constrained, as shown in Table 4 (The lower limits of x coordinate for P4 and P6 are set as the original values to maintain the basic geometric profile near the leading edge). The object is to improve lift-drag ratios under full conditions: 11 different attack angles from -5° to 15° with interval of 2° ($Re = 0.2 \times 10^6$, Ma = 0.06).

The objective functions and constraints are as follows:

$$F_1(X) = \sum_{i=0}^{10} (R_i - R_i^0) \tag{4}$$

$$F_2(X) = \frac{\sum_{i=0}^{10} \left(R_i - R_i^0 - \frac{F_1(X)}{11}\right)^2}{11} \tag{5}$$

$$R_i \geq R_i^0,\ i = -5, -3, \ldots, 15, \tag{6}$$

Where $F_1(X)$ is the sum of increments of lift-drag ratios under 11 different attack angles representing the performance improvement, and $F_2(X)$ is the variance of lift-drag ratios increments under 11 different attack angles representing performance proportionality. X represents the design variables (the coordinates of control points), R_i^0 and R_i represent the lift-drag ratios of the original and optimized airfoils respectively under the attack angle of i. In this optimization, the $F_1(X)$ is expected to be increased and $F_2(X)$ is expected to be decreased. The optimized lift-drag ratio under each attack angle should not be smaller than the original one (Eq. (6)).

The optimization process is illustrated in Fig. 8. The optimization starts from the control points of the original airfoil (Table 4), then the coordinates of the Bezier curves are generated by self-programming software 'BEZIER.exe' based on the coordinates of the control points. The aerodynamic performances are calculated by XFOIL.exe, and the result will be saved in designated text files. Finally, the lift and drag coefficients are obtained from the text files by Data Exchanger component, and the objective function $F_1(X)$ and $F_2(X)$ are calculated to provide feedback to Genetic Algorithm. The population size is 60, and the evolution generation is 60. The other parameters are set as default.

3.3. Results and discussion

In order to verify the accuracy of XFOIL, the aerodynamic performance of E387 calculated by XFOIL is compared with the experiment data [24], as shown in Fig. 9 (C_l is the lift coefficient, and C_d is the drag coefficient). The results from XFOIL and experiment are in good agreement with each other, which can meet the optimization requirement.

The population distribution is generated after 3601 runs as shown in Fig. 10, where ′ × ′ represents solution beyond constraints of Eq. (6). Two representative solutions were selected from the Pareto front which are named Opt-A ($F_1(X)$ = 103.6604614, $F_2(X)$ = 21.37950391) and Opt-B ($F_1(X)$ = 36.0164854, $F_2(X)$ = 1.189632905). The profile comparison between the original and the optimized airfoils (the coordinates of optimized control points are shown in Table 5) are displayed in Fig. 11, and the relative displacement of control point coordinates are illustrated in Fig. 12.

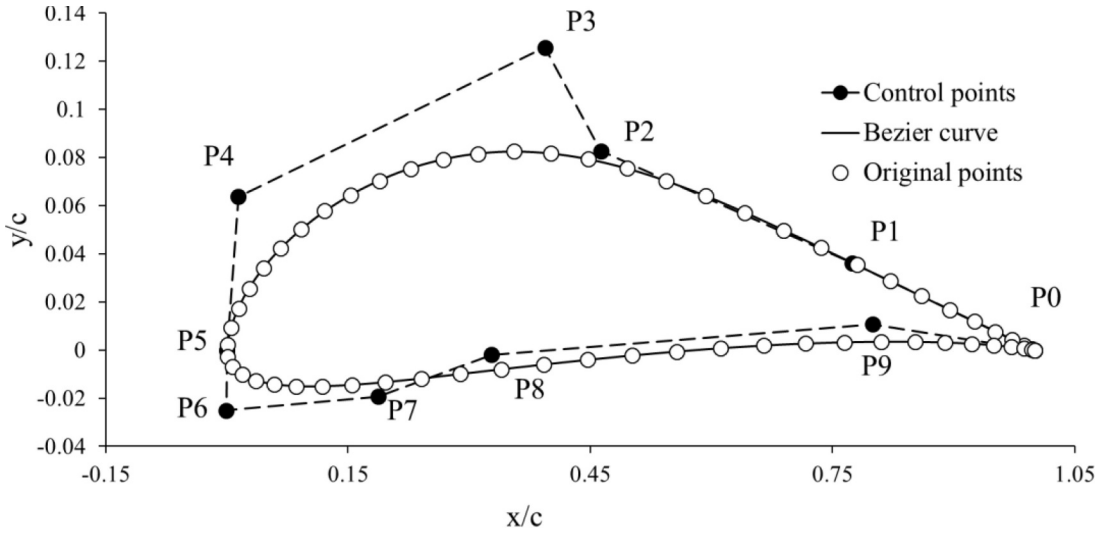

Fig. 7. Fitting curves of airfoil E387 by downhill simplex method.

Table 4
Variation range of control points.

control points for upper curve	Lower limit	Initial value	Upper limit	control points for lower curve	Lower limit	Initial value	Upper limit
P1*x*	0.674	0.773969293	0.874	P6*x*	−0.001073036	−0.001073036	0.099
P1*y*	0.026	0.036122616	0.046	P6*y*	−0.035	−0.025062025	−0.015
P2*x*	0.363	0.463096708	0.563	P7*x*	0.087	0.186959028	0.287
P2*y*	0.073	0.082727179	0.093	P7*y*	−0.029	−0.019384850	−0.009
P3*x*	0.294	0.393964529	0.494	P8*x*	0.227	0.327455044	0.427
P3*y*	0.116	0.125631601	0.136	P8*y*	−0.012	−0.001939915	0.008
P4*x*	0.014162857	0.014162857	0.114	P9*x*	0.699	0.799243450	0.899
P4*y*	0.054	0.063724995	0.074	P9*y*	0.001	0.010752819	0.021

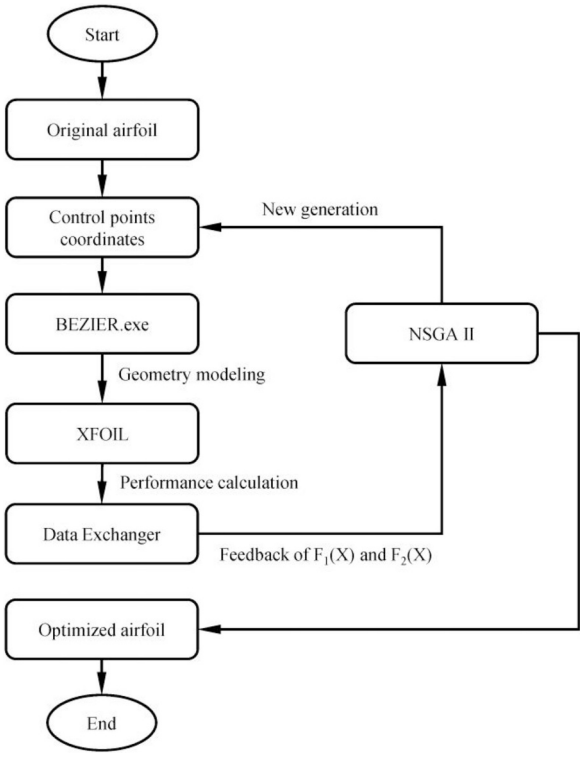

Fig. 8. Flow chart of optimization.

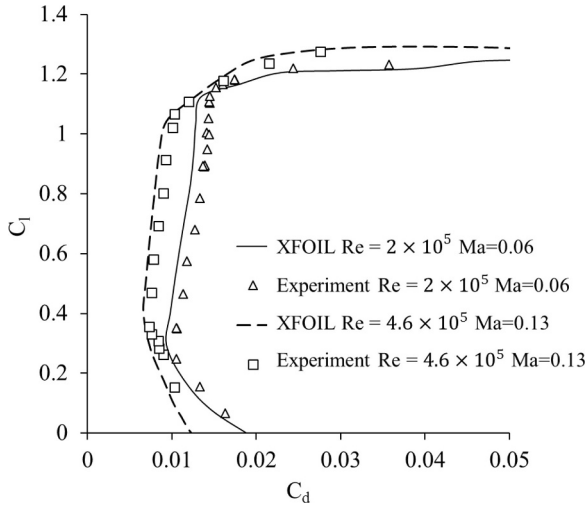

Fig. 9. Calculation result of E387 compared with experiment data.

The comparison of aerodynamic performance is displayed in Fig. 13, and the detailed information of lift-drag ratio increment is shown in Fig. 14. The lift-drag ratios of the optimized airfoils are both improved compared with the original airfoil, but they are improved in different aspects. Opt-A ($F_1(X)$ high, $F_2(X)$ high) alters the lift-drag ratio distribution relative to the attack angle: on the one hand, the lift-drag ratios under smaller attack angles are enhanced, on the other hand, the stall characteristics under large attack angles are ameliorated. Opt-B ($F_1(X)$ low, $F_2(X)$ low) maintains the original lift-drag ratio distribution of airfoil E387, with similar increment under different attack angles. Although the performance of Opt-B is inferior to Opt-A in conditions with larger or smaller attack angles, the performance is better in optimal condition with the attack angle of 7° The increment distribution of lift-drag ratio in Fig. 14 provides a clear demonstration of different focus of the two optimized airfoils.

The pressure coefficient distributions of the original and optimized airfoils under the attack angle of −1°, 3°, 7°and 9° are displayed in Fig. 15. For Opt-A, the pressure distributions are improved differently for different attack angles. For small and negative attack angles, the pressure near the front and rear part of the upper surface is significantly decreased, resulting in higher differential pressure between upper and lower surface, which is propitious to the increase of lift coefficient. For large attack angle, the adverse pressure gradient on the upper surface is decreased, which helps to postpone the generation of the separated flow. This is related to the higher lift coefficient and lower drag coefficient in Fig. 13. The pressure coefficient distribution of Opt-B is similar to E387, with modest increment of differential pressure between upper and lower surface under each attack angle.

The introduction of variance control in this research is an attempt to provide guidance for performance optimization from the perspective of full working conditions, and provide optimized low-Reynolds-number high-lift airfoils with different advantageous characteristics. The Opt-A type of solution is suitable for initial exploration while the Opt-B type of solution is suitable for final reinforcement.

4. Conclusion

A rapid closed-loop procedure for airfoil design and optimization is introduced in this research. According to the analysis mentioned above, several conclusions can be drawn as follows:

1 A rapid airfoil parameterization procedure based on Bezier curve and direct search method is provided as the pre-processing module of the multi-objective aerodynamic optimization. The Bezier curve is suitable for airfoil parameterization, and the shape of the upper and lower curves can be precisely and visually controlled by Bezier control points. The initial data generated by self-programming software 'Bezier Curve Fitting.exe' provides proper basement for direct search method, and the fitting process is finished with great

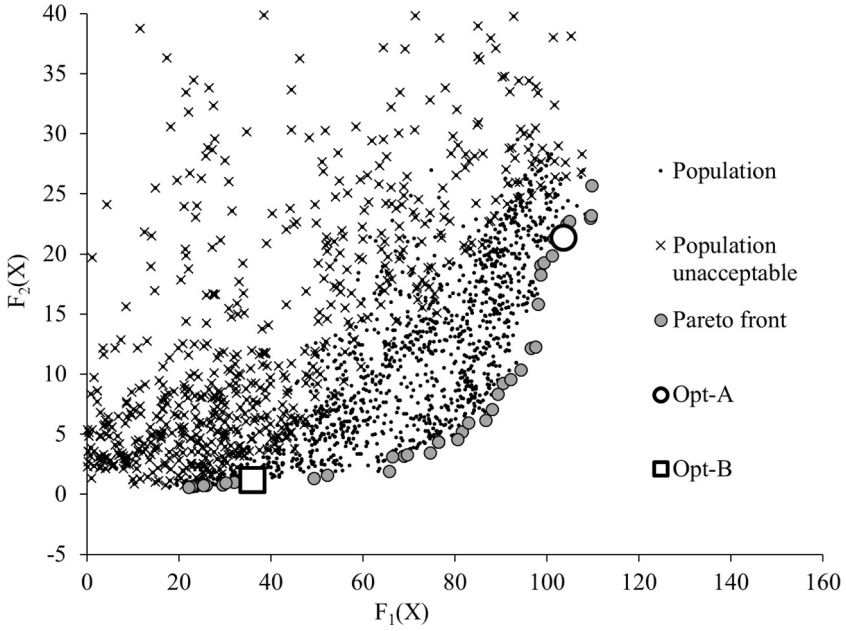

Fig. 10. Population distribution of optimization.

Table 5
Control points coordinates of Opt-A and Opt-B.

Control points	Opt-A	Opt-B	Control points	Opt-A	Opt-B
P1*x*	0.838349916	0.827711286	P6*x*	−0.000311457	−0.000282298
P1*y*	0.044640180	0.032510230	P6*y*	−0.029818565	−0.029788407
P2*x*	0.526207228	0.501807161	P7*x*	0.155730459	0.145335831
P2*y*	0.088560746	0.083656030	P7*y*	−0.021133157	−0.021129063
P3*x*	0.355068086	0.407127823	P8*x*	0.375997525	0.374158288
P3*y*	0.135897241	0.135657443	P8*y*	0.006939582	0.005723939
P4*x*	0.014516334	0.023004223	P9*x*	0.735333237	0.730101709
P4*y*	0.073370833	0.072161878	P9*y*	0.018218683	0.018227067

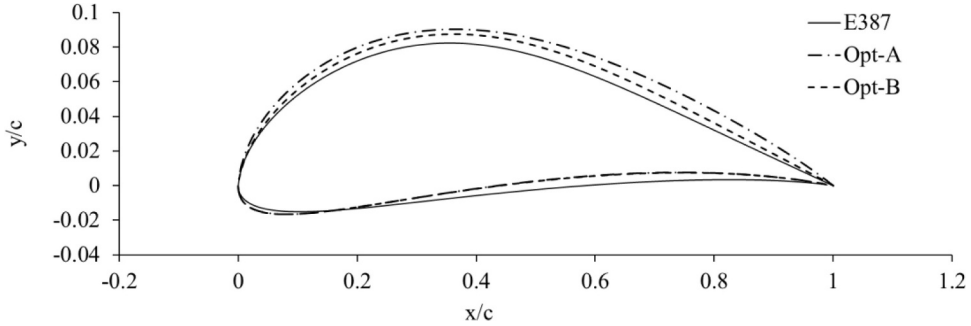

Fig. 11. Comparison of geometry between optimized and original airfoils.

speed and accuracy.

2 The application of XFOIL in performance calculation instead of CFD can enhance the optimization efficiency significantly with acceptable accuracy, and the removal of approximate model makes the optimization program more concise, which is beneficial to engineering application.

3 The aerodynamic performances under full working conditions of Opt-A and Opt-B are both improved by NSGA II algorithm. The lift-drag ratio of Opt-A is improved significantly under conditions of small and large attack angles, and the stall characteristics are ameliorated. The lift-drag ratio of Opt-B is enhanced synchronously under different attack angles, and the distribution characteristics are maintained. The introduction of variance control in the objective function enables the differentiation of the optimized solutions for different requirements in engineering application, which is of reference significance to the design and optimization of low-Reynolds-number airfoils.

Author statement

The submitted revised version titles "Research on parameterization and optimization procedure of low-Reynolds-number airfoils based on genetic algorithm and Bezier curve" was written by Dr Xuesong Wei, Miss Xiaoyang Wang and Prof. Songying Chen. Prof. Chen is the

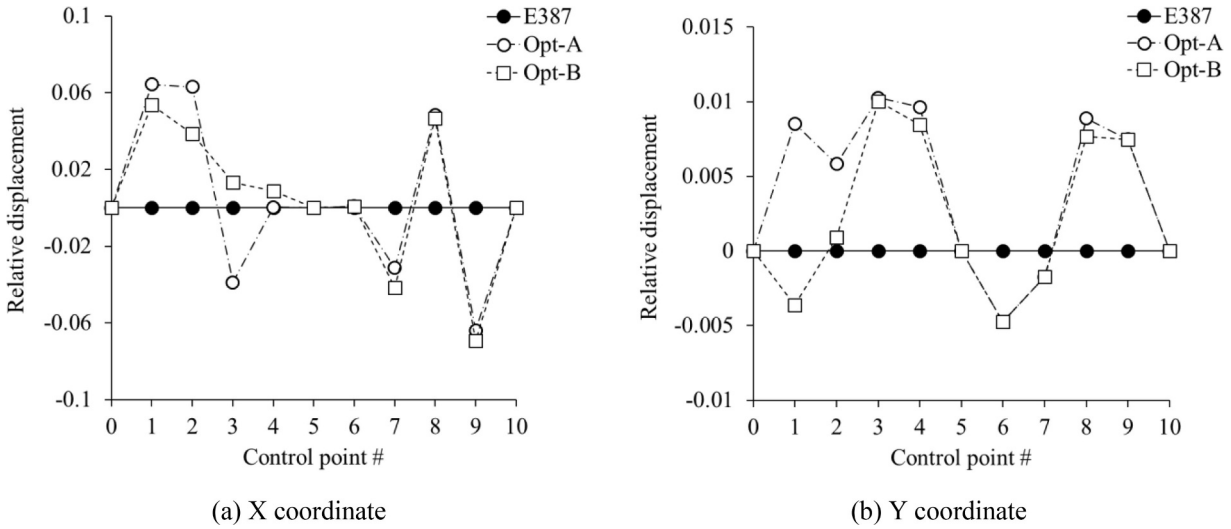

Fig. 12. Displacement of optimized control points relative to original ones. (a) X coordinate, (b) Y coordinate.

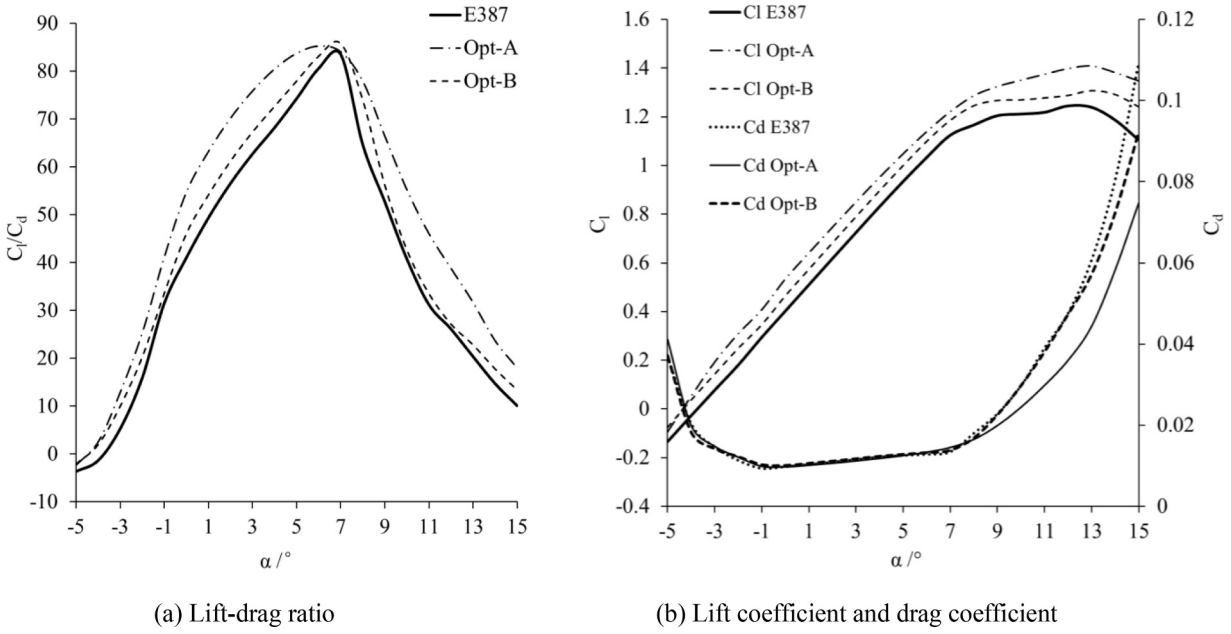

Fig. 13. Comparison of aerodynamic performance between optimized and original airfoils. (a) Lift-drag ratio, (b) Lift coefficient and drag coefficient.

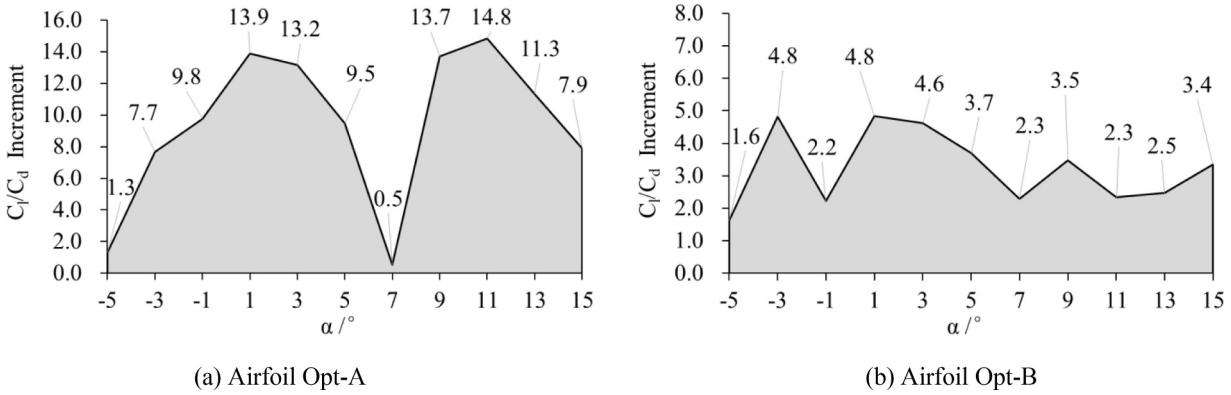

Fig. 14. Increment of lift-drag ratio under different attack angles. (a) Airfoil Opt-A, (b) Airfoil Opt-B.

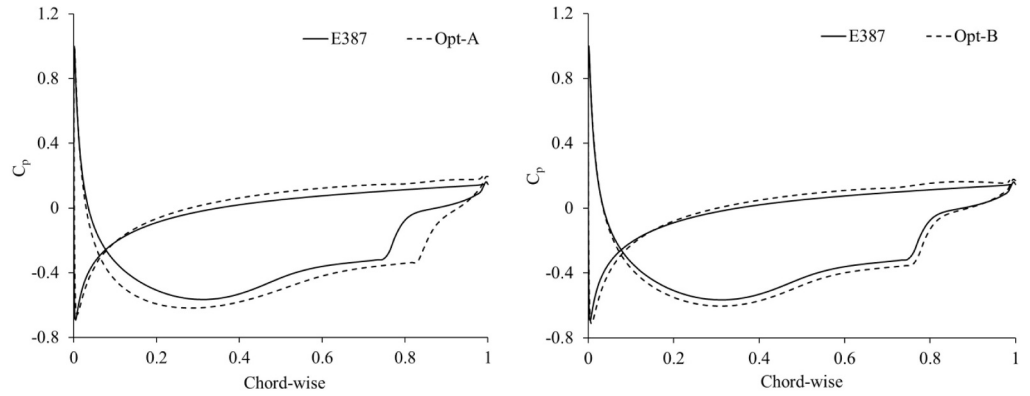

(a) α =-1° Opt-A vs E387

(b) α =-1° Opt-B vs E387

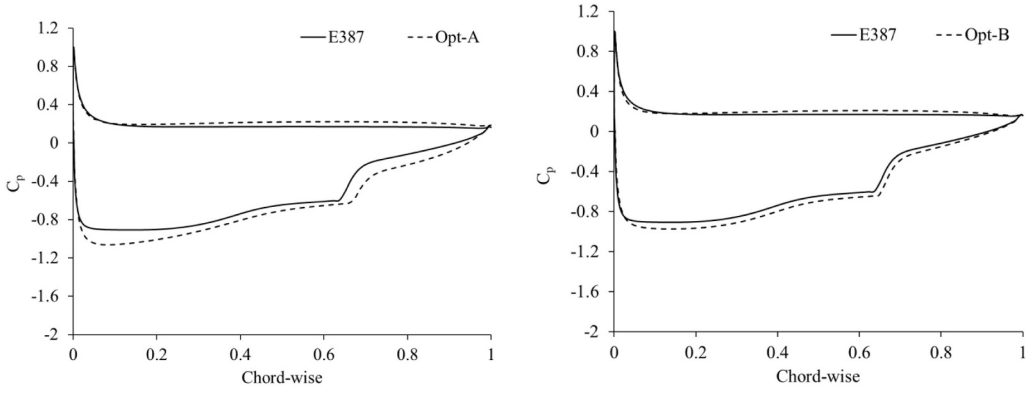

(c) α =3° Opt-A vs E387

(d) α =3° Opt-B vs E387

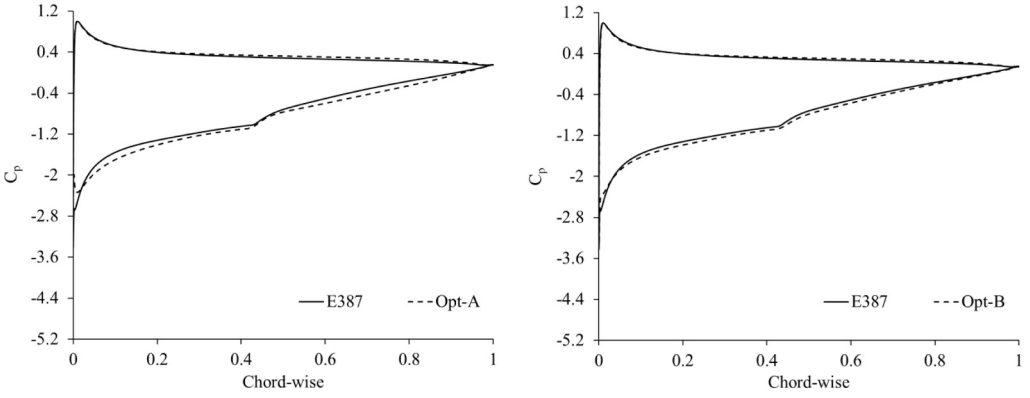

(e) α =7° Opt-A vs E387

(f) α =7° Opt-B vs E387

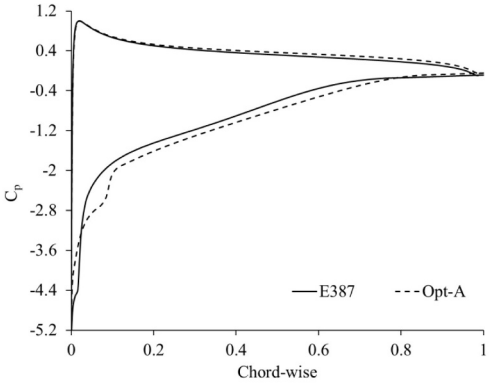

(g) α =11° Opt-A vs E387

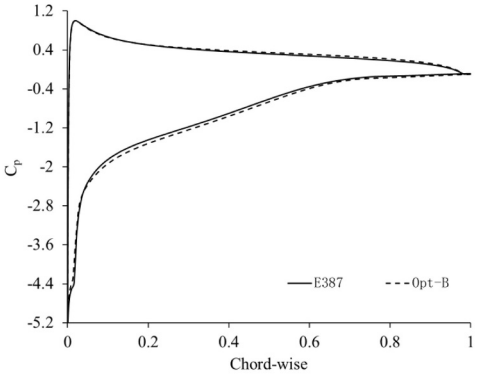

(h) α =11° Opt-B vs E387

Fig. 15. Comparison of pressure coefficient between optimized and original airfoils, (a) $\alpha = -1^\circ$ Opt-A vs E387, (b) $\alpha = -1^\circ$ Opt-B vs E387, (c) $\alpha = 3^\circ$ Opt-A vs E387, (d) $\alpha = 3^\circ$ Opt-B vs E387, (e) $\alpha = 7^\circ$ Opt-A vs E387, (f) $\alpha = 7^\circ$ Opt-B vs E387, (g) $\alpha = 11^\circ$ Opt-A vs E387, (h) $\alpha = 11^\circ$ Opt-B vs E387.

Correspondance author. Dr Wei made substantial contributions to the conception of the work and numerical results. Xiaoyang presented the algorithm code and analysis to the work. Prof. Chen gave the frame of the manuscript and double checked the revised version.

Declaration of Competing Interest

The authors declare that they have no known competing financial interests or personal relationships that could have appeared to influence the work reported in this paper.

Acknowledgements

This research was supported by the National Natural Science Foundation of China (Grant No. 51906126), the Key Laboratory of High-efficiency and Clean Mechanical Manufacture at Shandong University, Ministry of Education, the Fundamental Research Funds of Shandong University (Grant No. 2018GN007) and Ocean Industry Leading Talent Team of Yantai's “Double Hundred Plan”.

References

[1] Bedon G, Betta S D, Benini E. Performance-optimized airfoil for Darrieus wind turbines. Renew Energy 2016;94:328–40.
[2] Daróczy L, Janiga G, Thévenin D. Computational fluid dynamics based shape optimization of airfoil geometry for an H-rotor using a genetic algorithm. Eng Optim 2018;50(9):1483–99.
[3] Luo X, Zhu G, Feng J. Multi-point design optimization of hydrofoil for marine current turbine. J Hydrodyn. Ser B 2014;26(5):807–17.
[4] Jeong JH, Kim SH. Optimization of thick wind turbine airfoils using a genetic algorithm. J Mech Sci Technol 2018;32(7):3191–9.
[5] Huang B, Zhu GJ, Kanemoto T. Design and performance enhancement of a bi-directional counter-rotating type horizontal axis tidal turbine. Ocean Eng 2016;128:116–23.
[6] Ram KR, Lal SP, Ahmed MR. Design and optimization of airfoils and a 20 kW wind turbine using multi-objective genetic algorithm and HARP_Opt code. Renew Energy 2019;144:56–67.
[7] Zhang T, Huang W, Wang Z, et al. A study of airfoil parameterization, modeling, and optimization based on the computational fluid dynamics method. J. Zhejiang Univ-Sci A 2016;17(8):632–45.
[8] Jones BR, Crossley WA, Lyrintzis AS. Aerodynamic and aeroacoustic optimization of rotorcraft airfoils via a parallel genetic algorithm[J]. J Aircr 2000;37(6):1088–96.
[9] Obayashi S, Takahashi S, Fejtek I. Transonic wing design by inverse optimization using MOGA. Sixth Annual Conference of the Computational Fluid Dynamics Society of Canada. 1998.
[10] Liu Z, Dong L, Moschetta JM. Optimization of nano-rotor blade airfoil using controlled elitist NSGA-II. Int J Micro Air Veh 2014;6(1):29–42.
[11] DRELA M, GILES MB. Viscous-inviscid analysis of transonic and low Reynolds number airfoils. AIAA J 1987;25(10):1347–55.
[12] Drela M. XFOIL: an analysis and design system for low Reynolds number airfoils. Low Reynolds number aerodynamics. Berlin, Heidelberg: Springer; 1989. p. 1–12.
[13] Molland AF, Bahaj AS, Chaplin JR. Measurements and predictions of forces, pressures and cavitation on 2-D sections suitable for marine current turbines. Proceedings of the Institution of Mechanical Engineers Part M. J Eng Maritime Environ 2004;218(2):127–38.
[14] Morgado J, Vizinho R, Silvestre MAR, et al. XFOIL vs CFD performance predictions for high lift low Reynolds number airfoils. Aerosp Sci Technol 2016;52:207–14.
[15] Timmer WA, van Rooy R. Thick airfoils for HAWTs. J Wind Eng Ind Aerodyn 1992;39(1–3):151–60.
[16] Ronsten G. Static pressure measurements on a rotating and a non-rotating 2.375 m wind turbine blade. Comparison with 2D calculations. J Wind Eng Ind Aerodyn 1992;39(1–3):105–18.
[17] Gunasekaran M, Mukherjee R. Behaviour of trailing wing(s) in echelon formation due to wing twist and aspect ratio. Aerosp Sci Technol 2017;63:294–303.
[18] Koch PN, Evans JP, Powell D. Interdigitation for effective design space exploration using iSIGHT. Struct Multidis Optim 2002;23(2):111–26.
[19] Kharal A, Saleem A. Neural networks based airfoil generation for a given Cp using Bezier–PARSEC parameterization. Aerosp Sci Technol 2012;23(1):330–44.
[20] Hooke R, Jeeves TA. “Direct Search” solution of numerical and statistical problems. J ACM (JACM) 1961;8(2):212–29.
[21] Nelder JA, Mead R. A simplex method for function minimization. Comput J 1965;7(4):308–13.
[22] Holland J.H. Adaptation in natural and artificial systems:an introductory analysis with applications to biology, control, and artificial intelligence. University of Michigan Press, 1975.
[23] Deb K, Agrawal S, Pratap A, et al. A fast elitist non-dominated sorting genetic algorithm for multi-objective optimization: NSGA-II. Parallel Problem Solving from Nature PPSN VI 2000:849–58.
[24] Mcghee R.J., .Walker B.S., .Millard B.F. Experimental results for the Eppler 387 airfoil at low Reynolds numbers in the Langley Low-Turbulence Pressure Tunnel. NASA Tech Memo, 1988.